**Biophysical Journal, Volume *120***

## Supplemental information

# The key role of solvent in condensation: Mapping water in liquid-liquid phase-separated FUS

**Jonas Ahlers, Ellen M. Adams, Verian Bader, Simone Pezzotti, Konstanze F. Winklhofer, Jörg Tatzelt, and Martina Havenith**

## Supporting Information to

# The key role of solvent in condensation: Mapping hydration water in liquid-liquid phase-separated FUS

J. Ahlers, E. M. Adams, V. Bader, S. Pezzotti, K. F. Winklhofer, J. Tatzelt, M. Havenith

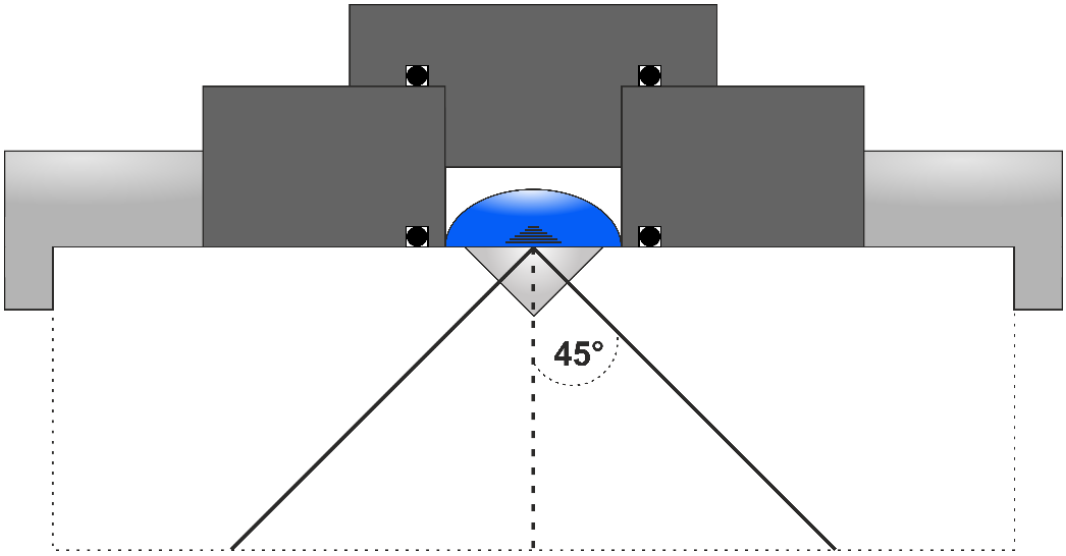


***Figure S1. Schematic drawing of the cross-section of the liquid sample cell.*** *A polyvinyl chloride (PVC) disk is placed on top of the diamond prism (grey triangle) and fixed on the ATR unit by a metal support plate. The sample is pipetted on the crystal and the sample chamber is closed using a PVC top piece. To avoid leakage, o-rings are placed in a cavity next to the sample. Incoming light is incident at the crystal surface at* $\theta$*=45° resulting in total internal reflection. The evanescent wave penetrates the sample and is then reflected towards the detector.*

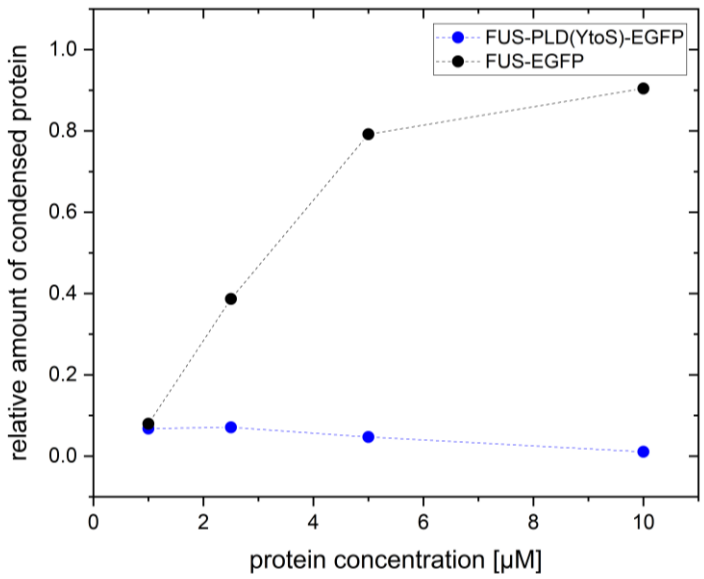


***Figure S2. FUS-EGFP provides robust phase separation at concentrations bigger than 5 µM.*** *To determine the amount of condensed protein, microscopy images of 1, 2.5, 5 and 10 µM FUS-EGFP and FUS-PLD(YtoS)-EGFP solutions were analyzed using the Fiji software (1). For the FUS-EGFP solution an image size of 310x310 µm was analyzed by applying a threshold to create a selection of the droplet areas. The fluorescence signal was measured for the droplet and the whole image area and the ratio was taken to obtain the relative amount of condensed protein. For the FUS-PLD(YtoS)-EGFP samples the same analysis was performed based on images with a size of 50x50 µm.*

## Spectral Deconvolution of FUS-EGFP ATR Absorption Spectra

The Δα spectra of the 10 µM FUS-EGFP can be modeled as the sum of damped harmonic oscillator functions (2), as shown in Equation S1

$$\Delta\alpha = \sum_{n=1}^{N} \frac{A_n \omega_{0,n} v}{4\pi^3 \left[ \frac{v^2 \omega_{0,n}^2}{\pi^2} + \left( v_{d,n}^2 + \frac{\omega_{0,n}^2}{4\pi^2} - v^2 \right)^2 \right]} \quad \text{(S1)}$$

Where $A_n$, $\omega_{0,n}$, and $v_{d,n}$ describe the amplitude, width, and center frequency of the $n^{th}$ resonance. The unperturbed center frequency, $v_{0,n}$, can be determined from the relation $v_{0,n} = \sqrt{v_{d,n}^2 + \frac{\omega_{0,n}^2}{4\pi^2}}$. The damped harmonic linewidth is related to the oscillator's dipole moment autocorrelation function through $\tau = \frac{1}{\omega_{0,n} c}$, where c is the speed of light. The damped harmonic oscillator fit and the corresponding fit parameters are shown in Figure S1 and Table S1, respectively.

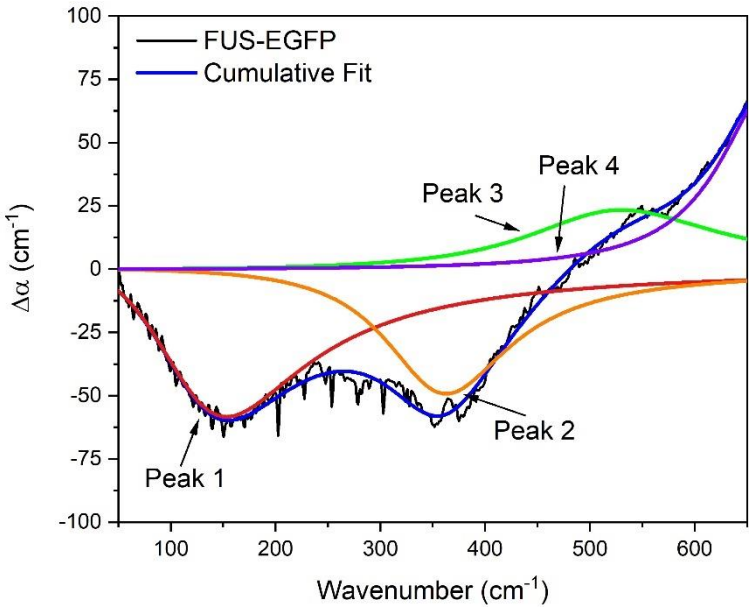


***Figure S3. FUS-EGFP Δα spectrum can be fitted by four harmonic oscillators.*** *Results of damped harmonic oscillator fitting of the Δα spectrum of 10 µM FUS-EGFP (see Table S1 for an overview of the fitted parameters).*

***Table S1. Fitting parameters of the ATR-FTIR Δα of 10 µM FUS-EGFP LLPS droplets.*** *The perturbed and unperturbed peak frequency, as well as the line width, are given in $cm^{-1}$, while the lifetime is given in fs.*

| | $\nu_d$ | $\nu_0$ | A | $\omega_0$ | $\tau$ |
|---|---|---|---|---|---|
| 10 µM FUS-EGFP | | | | | |
| Peak 1 | 126 ± 1 | 155 ± 3 | -748 ± 7 | 563 ± 11 | 59 ± 4 |
| Peak 2 | 356 ± 1 | 364 ± 3 | -709 ± 42 | 485 ± 25 | 69 ± 9 |
| Peak 3 | 518 ± 10 | 530 ± 22 | 293 ± 65 | 700 ± 161 | 47 ± 42 |
| Peak 4 | 674 ± 23 | 677 ± 46 | 928 ± 286 | 402 ± 110 | 82 ± 50 |

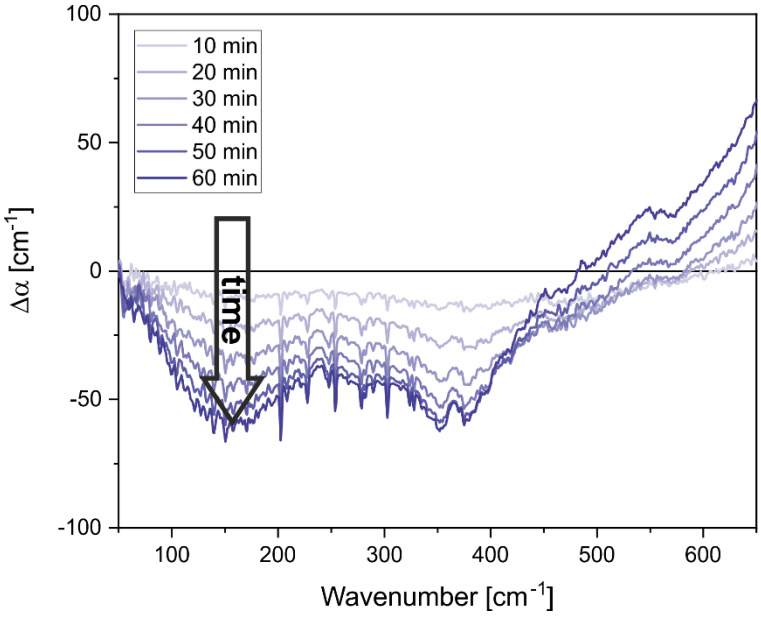


***Figure S4. Intensity of the spectral fingerprint (Δa) of phase-separated FUS increases over time.*** *Comparison of 10 µM FUS-EGFP Δα spectra at 10, 20, 30, 40, 50, and 60 min (from bright to dark blue).*

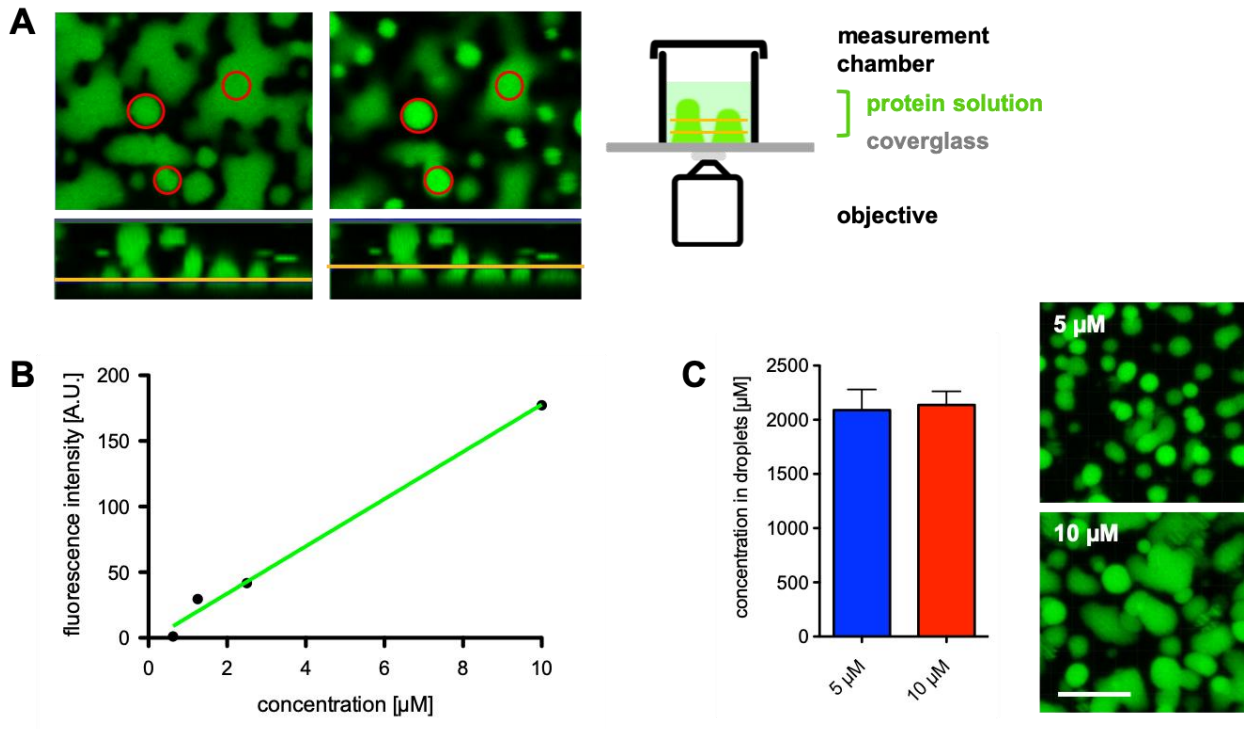


***Figure S5. Final FUS-EGFP concentration in droplets does not depend on the starting protein concentration.*** *For the determination of the protein concentration within the droplets, 2 confocal planes (yellow lines) at different heights were chosen and the data was averaged as shown here for 10 µM FUS-EGFP 1 h after TEV cleavage* ***(A)****. Based on the fluorescence intensity of a dilution series of uncut FUS-EGFP* ***(B)****, the final concentration was calculated for each sample at the indicated concentration 1 h after TEV cleavage* ***(C)****. Scale bar = 6 µm*

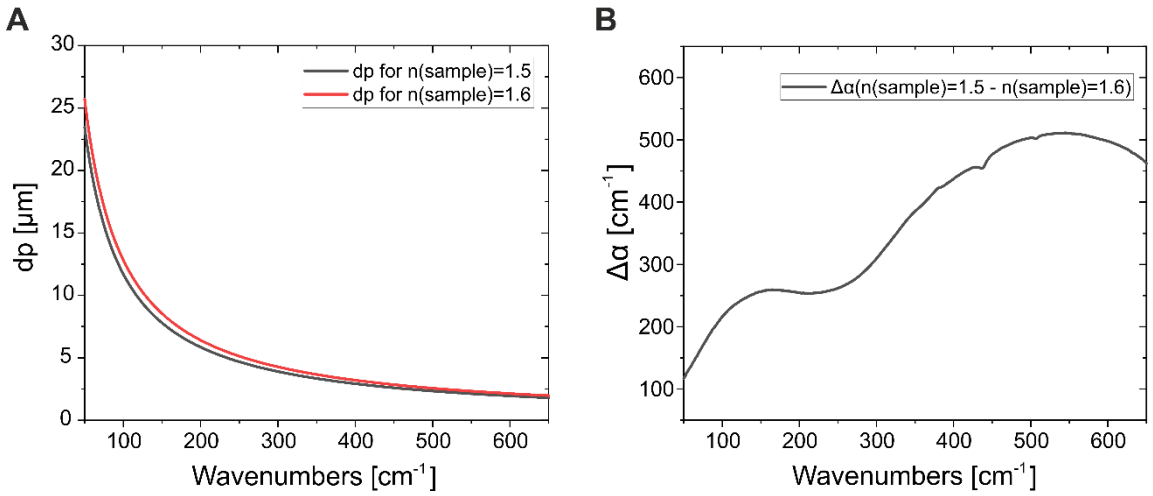


***Figure S6. Influence of refractive index on the calculated Δα spectra.*** *The penetration depth (dp) for $n_{sample}$=1.5 and 1.6 were calculated using Equation 2 and plotted together over the frequency range of 50-650 cm$^{-1}$* ***(A)****. An increase of the penetration depth can be seen over all frequencies for the higher refreactive index. A buffer spectrum was used to visualize the effect of an increase in refractive index on the resulting Δα spectrum* ***(B)****.*

## Spectral Deconvolution of Water ATR Absorption Spectra

The Δα spectra of water can also be modeled by Equation S1. The damped harmonic oscillator fit and the corresponding fit parameters are shown in Figure S4 and Table S2, respectively.

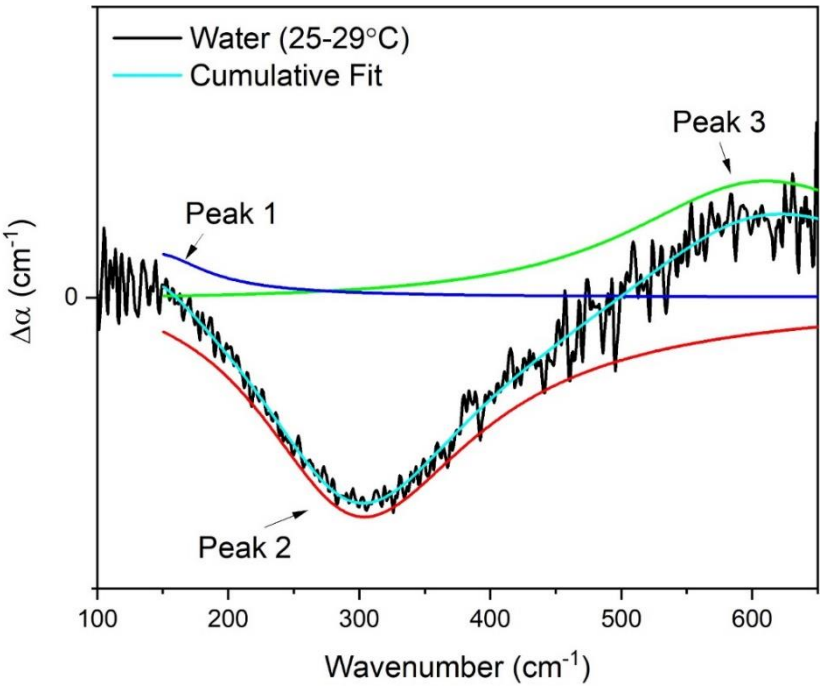


***Figure S7: Δα spectrum of water at 25 °C minus water at 29 °C can be fitted by three harmonic oscillators.*** *Results of damped harmonic oscillator fitting of the Δα spectrum of water at 25 °C minus water at 29 °C.*

***Table S2. Fitting parameters of the ATR-FTIR Δα of water (25-29 °C).*** *The perturbed and unperturbed peak frequency, as well as the line width, are given in $cm^{-1}$, while the lifetime is given in fs.*

| | $\nu_d$ | $\nu_0$ | A | $\omega_0$ | $\tau$ |
|---|---|---|---|---|---|
| Water | | | | | |
| Peak 1 | 140 ± 37 | 146 ± 72 | 190 ± 67 | 262 ± 143 | 127 ± 99 |
| Peak 2 | 287 ± 3 | 304 ± 2 | -856 ± 19 | 626 ± 26 | 53 ± 8 |
| Peak 3 | 596 ± 4 | 610 ± 2 | 503 ± 11 | 832 ± 77 | 40 ± 17 |

## ATR vs. Transmission Spectra of Water in THz Regime

Ultrapure water was measured at room temperature and the resulting $\alpha_{ATR}$ spectrum is plotted together with an $\alpha_{Transmission}$ spectrum of water at 25 °C taken from Bertie et al (3). The H-bond stretch mode and librational mode are red shifted in the ATR spectrum with respect to the transmission spectrum.

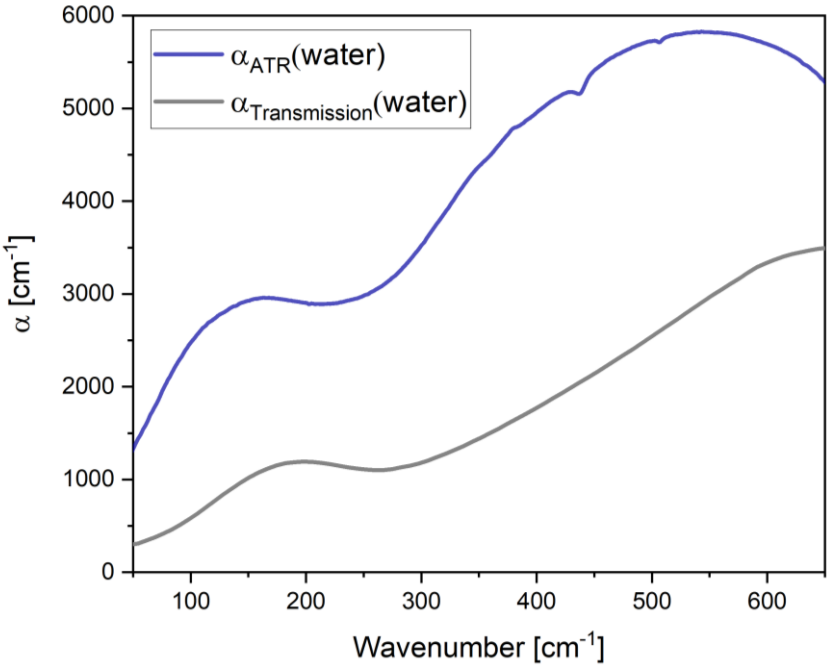


***Figure S8. The ATR spectrum of water (blue) in the THz region is red-shifted compared to the transmission spectrum (grey).*** *Comparison of the α spectra of water in ATR and in transmission (3) in the range of 50 to 650 $cm^{-1}$.*

## Volume Exclusion Estimation

Assuming negligible absorption of the protein itself, the Δα spectral amplitude corresponding to pure solvent volume exclusion, where the volume of solvent excluded equals the volume of the protein solute, can be estimated from the relation $\Delta\alpha = (V_{protein}/V_{total})^* \alpha_{buffer} - \alpha_{buffer}$ (4).

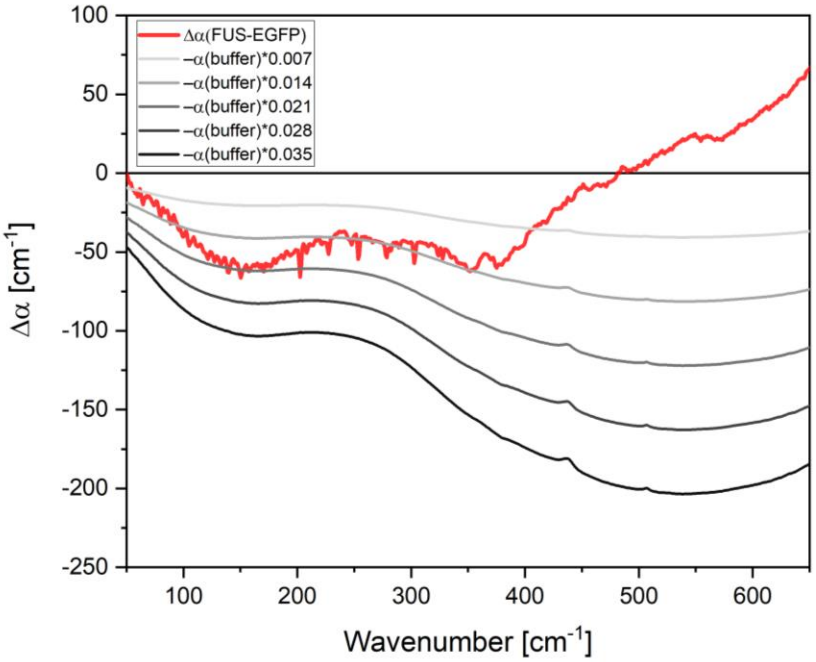


***Figure S9. Negative 155 cm$^{-1}$ peak of phase-separated FUS Δα spectrum cannot be explained solely by water loss due to volume exclusion.*** *Comparison of Δα spectrum of 10 µM FUS-EGFP after 60 min (red) to the negative ATR buffer spectra sclaed by different protein volume factors (light grey to black: 0.7, 1.4, 2.1, 2.8, and 3.5 %).*

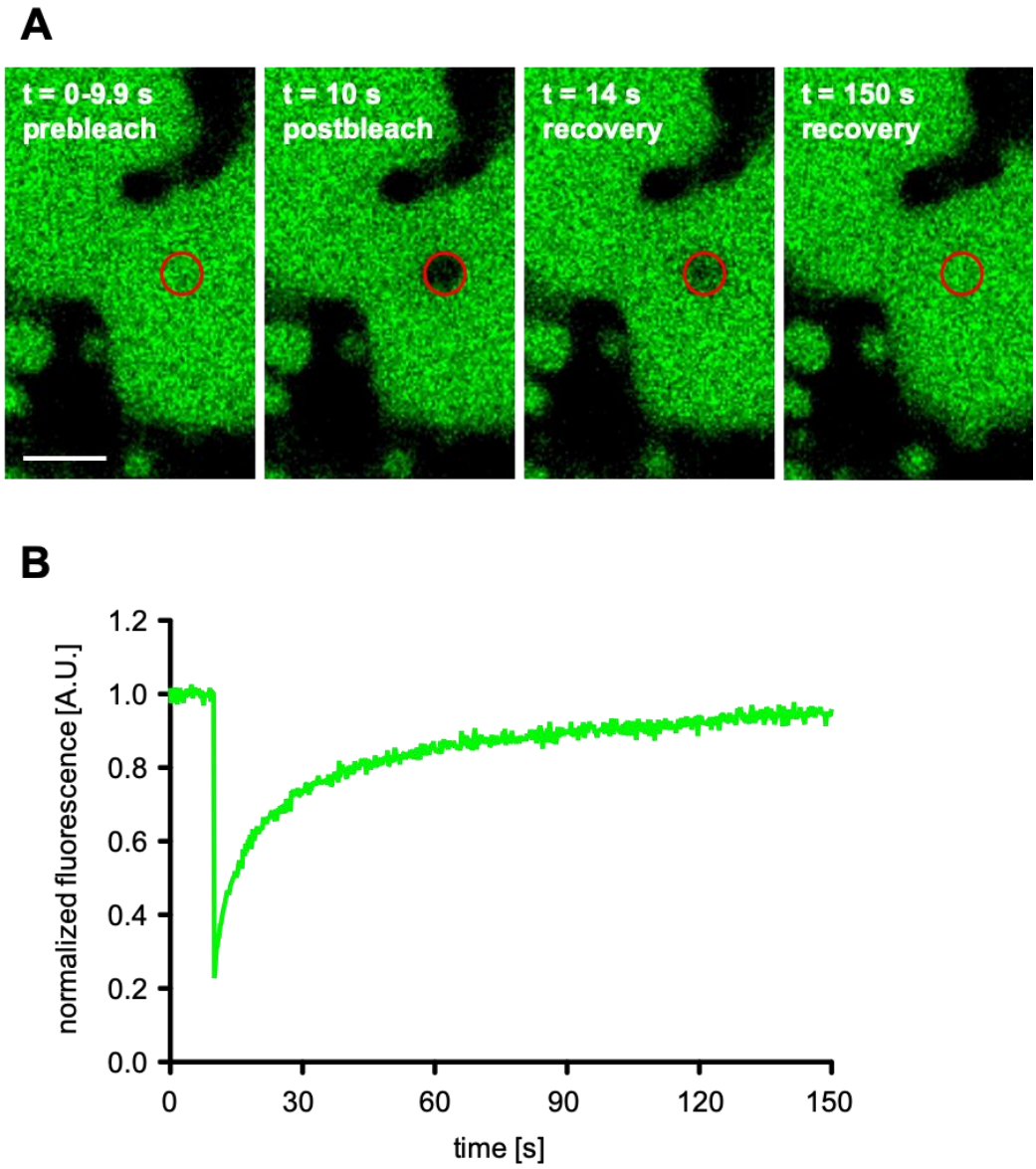


***Figure S10. Fluorescent recovery after photobleaching (FRAP) in FUS-EGFP droplets indicates a high protein mobility.*** *For the determination of the 10 µM FUS-EGFP 1 h after TEV cleavage, protein mobility within the droplets was measured by FRAP.* ***A:*** *After 10 s of baseline recording (prebleach), a small area of interest (AOI; red circle) was photobleached (t=10 s; postbleach). Within 4 s (t=14 s; recovery) approx. 50% of the fluorescence intensity was recovered, almost complete recovery was detected after 150 s.* ***B:*** *The average normalized fluorescence intensity of three AOIs was plotted over time.*

## References


1. Schindelin, J., I. Arganda-Carreras, E. Frise, V. Kaynig, M. Longair, T. Pietzsch, S. Preibisch, C. Rueden, S. Saalfeld, B. Schmid, J.-Y. Tinevez, D. J. White, V. Hartenstein, K. Eliceiri, P. Tomancak, and A. Cardona. 2012. Fiji: an open-source platform for biological-image analysis. Nature methods 9:676–682.
2. Schwaab, G., F. Sebastiani, and M. Havenith. 2019. Ion Hydration and Ion Pairing as Probed by THz Spectroscopy. Angewandte Chemie (International ed. in English) 58:3000–3013.
3. Bertie, J. E., and Z. Lan. 1996. Infrared Intensities of Liquids XX: The Intensity of the OH Stretching Band of Liquid Water Revisited, and the Best Current Values of the Optical Constants of H 2 O(l) at 25°C between 15,000 and 1 cm −1. Appl Spectrosc 50:1047–1057.
4. Ebbinghaus, S., S. J. Kim, M. Heyden, X. Yu, U. Heugen, M. Gruebele, D. M. Leitner, and M. Havenith. 2007. An extended dynamical hydration shell around proteins. Proceedings of the National Academy of Sciences of the United States of America 104:20749–20752.